III ECCOMAS THEMATIC CONFERENCE ON SMART STRUCTURES AND MATERIALS
W. Ostachowicz, J. Holnicki-Szulc, C. Mota Soares *et al.* (Eds.)
Gdansk, Poland, 9-11 July 2007

FLUX DENSITY VARIATION IN MAGNETORHEOLOGICAL FLUID DEVICES

Grzegorz Mikulowski[*] and David C. Batterbee[†]

[*]Smart-Tech Centre, Institute of Fundamental Technological Research, ul. Swietokrzyska 21, 00-049 Warsaw, Poland
email: gmikulow@ippt.gov.pl

[†]Department of Mechanical Engineering, The University of Sheffield, Sheffield, S1 3JD, UK
e-mail: d.batterbee@sheffield.ac.uk, web page: www.shef.ac.uk/mecheng

Keywords: magnetorheological, smart fluid, variable yield stress, modelling, large valve gap

Abstract *This paper presents an example where there is significant flux density variation across the valve gap of magnetorheological devices. Consequently, the MR fluid yield stress distribution cannot be assumed as constant in numerical modelling. In this paper, conventional MR fluid flow models are updated to account for quadratic yield stress distributions. The updated model is validated experimentally on a flow mode test rig that was designed for parallel flat plate flow. In general, it is shown that the effect of the yield stress variation is significant, and simplified models cannot predict the behaviour accurately. The presented model is shown to improve the numerical predictions of the experimental response.*

1 INTRODUCTION

In most papers devoted to the analysis of steady flow in MR fluids, authors assume invariable distribution of the magnetic flux across the valve gap[1, 2]. The assumption is valid for a significant number of the MR devices in which the dimension of the gap is small and the field intensity is high. However, in the case when the flux density variation is significant and cannot be assumed as constant, conventional models will not predict the behavior accurately. Such cases are more likely to occur in devices where the gap size is large. The conventional models of quasi-steady MR fluid flow are derived on the basis of the Bingham plastic flow equation. Here, the yield stress in the fluid is often assumed as constant across the valve gap. This is shown schematically in Figure 1(a), which depicts MR fluid flow between parallel flat plates of length l, and separated by distance h. The flow is excited by a pressure drop ΔP and magnetic flux ϕ. Assuming one-dimensional steady flow, and neglecting gravitational and compressibility effects, the following governing equation can be readily derived [3]:

$$\frac{\Delta P}{l} = \frac{d\tau}{dy} \tag{1}$$

Here, τ is the shear stress, and y is the vertical displacement coordinate across the gap. As shown in Figure 1, this implies a linear shear stress distribution, which is equal to zero at the centre of the channel. Due to the yield stress in the fluid, this leads to the development of a plug where the shear stress does not exceed this value. Outside of the plug, the fluid behaves in a viscous manner. In this paper, the most important modification to the conventional model is the introduction of a variable yield stress across the valve gap. This is shown in Figure 1(b) which indicates a quadratic distribution of the yield stress τ_y. This variation in τ_y can significantly reduce the flow rate for a given pressure drop. With reference to Figure 1(b), this is because the difference between the shear and yield stress, and hence the strain rate is lower. Consequently, the aim of this paper is to compare conventional and modified MR flow models with an experimental test rig that has notable variations in yield stress.

The paper begins with a review of the literature in this field. Next, the test facility is described, and the extent of the yield stress variation is validated by performing a finite element analysis of the magnetic circuit. MR fluid flow equations are then derived that account for this behavior. Finally, the new model is compared to both experimental data and a conventional model that assumes constant yield stress.

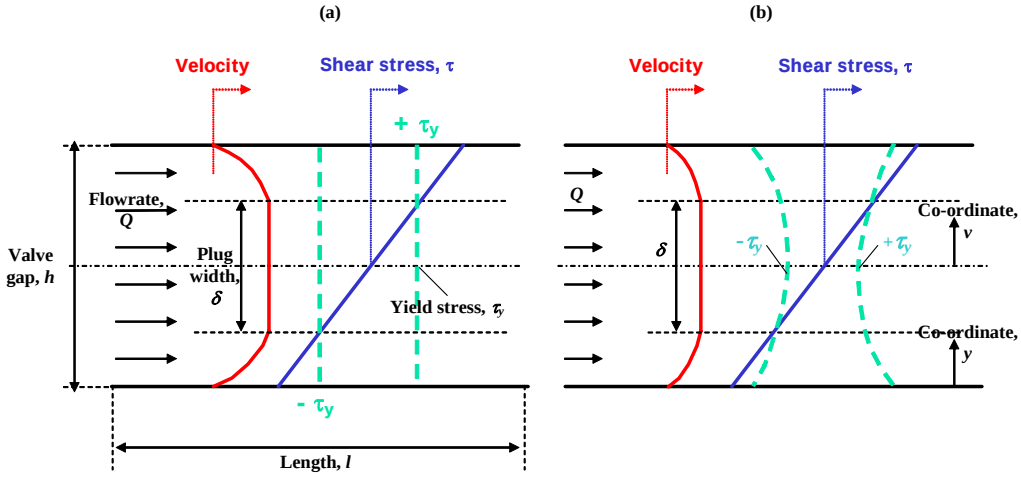

Figure 1: Schematic diagrams of MR fluid flow between parallel flat plates. (a) Constant yield stress distribution across the gap and (b) quadratic yield distribution across the gap.

2 LITERATURE REVIEW

The modelling of MR fluid behaviour under steady flow conditions is a widely considered problem[3-6], and can be used as the basis for the design and development of many applications with MR fluid. The most commonly considered constitutive model of MR fluid behaviour is a Bingham plastic body with the yield stress level varying dependently on the applied

magnetic field intensity. This way of modelling has proved its usefulness in characterisation, and the preliminary scaling of many adaptive devices based on MRF[1, 7, 8].

Bingham fluids are characterised by a yield stress, which must be exceeded in order to develop flow in the medium. Below the yield stress level the medium behaves like a solid body. The Bingham constitutive law was used to develop a dimensionless model of quasi-steady ER fluid flow between parallel flat plates[2]. Wereley developed a similar dimensionless form but using different dimensionless coefficients[3]. Models based on Bingham plastic behaviour have been successfully used to design experimental ER[1]and MR[9] dampers. The model has also served as a method of analysis for other classes of ER/MR devices. For example, equations were derived and validated experimentally to model steady flow for three modes of operation[3] - flow mode (e.g. valves, dampers), shear mode (e.g.clutches, brakes) and mixed mode.

There are some limitations to the quasi-steady Bingham plastic model. For example, the model has been observed to break down at high shear rates due to shear thickening/thinning behaviour. This has led researchers to look at alternative nonlinear models e.g. the Herschel-Bulkley constitutive law[6, 10]. The model can also break down at very low shear rates, which has led to the development of biviscous models that can account for behaviour in the pre-yield region[5].

Another important problem that is rarely considered is the magnetic field characterisation perpendicular to the fluid gap. In many of the investigations described above, the magnetic flux density and hence yield stress is assumed to be constant across the entire flow area. This assumption is valid in a wide class of devices that have the orifice gap small in comparison to the volume of magnetic circuit material but there may be instances when the assumption is not valid.

Transverse variation of the magnetic field in the gap was reported as the general analytical issue that can influence the character of flow in MR fluid ducts[9]. The authors developed an axisymmetric model that accounted for a variable yield stress by using an inverse power law. This was compared to a simplified model that assumed a constant yield stress, although the simplified model was found to be adequate for that problem.

In summary, the distribution of the magnetic field intensity is not a widely considered problem. Nevertheless, it is an important issue to be analysed in the case of potential devices where the fluidic gap must be designed larger, and then the predictions of the ER/MR fluid behaviour require a magnetic field intensity analysis perpendicular to the valve gap. Such a case is analysed both numerically and experimentally in the present investigation.

3 EXPERIMENTAL SETUP

3.1 Description of the test facility

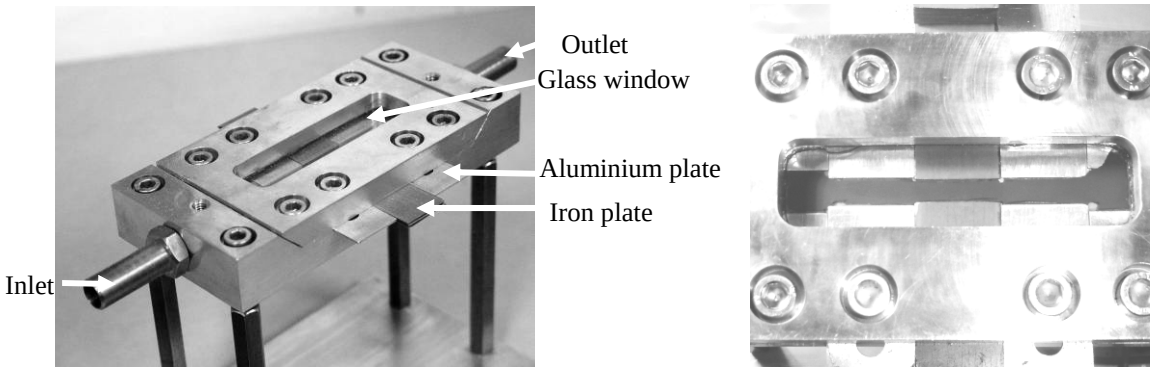

Figure 2: Overview of the experimental valve

In order to perform the research on the MRF in the flow mode, an experimental model of a magnetic valve was designed and fabricated (Figure 2(a)). The magnetic valve was designed in a way to enable the following measurements: determination of pressure drop variation as a function of the magnetic field intensity and visualization of the MR fluid in flow mode.

The experimental volume of the MR flow channel that was activated by the magnetic field was a rectangular block as shown in Figure 3. The fluid in the channel was excited with the magnetic field lines along the Y axis and the fluid was under a pressure gradient along the X axis (Figure 3). The dimensions of the channel were: 1 mm height, 3 mm width and the magnetically active length was 20 mm. Figure 2(b) presents the top view of the experimental valve. The top surface of the device is made of glass in order to enable the MR fluid flow observations. The dark grey area visible in Figure 2(b) represents the MR fluid. The channel's side borders are six plates. Four of them are aluminum plates (having non-magnetic properties) and two of them are made of silicon iron and play the role of magnetic poles, connected to the magnetic circuit (Figure 4).

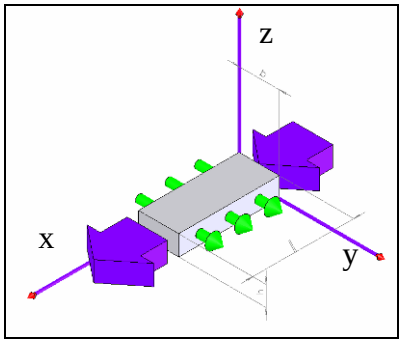

Figure 3: Geometrical representation of the active volume of the MR fluid, round arrows – magnetic induction, rectangular arrows – pressure gradient.

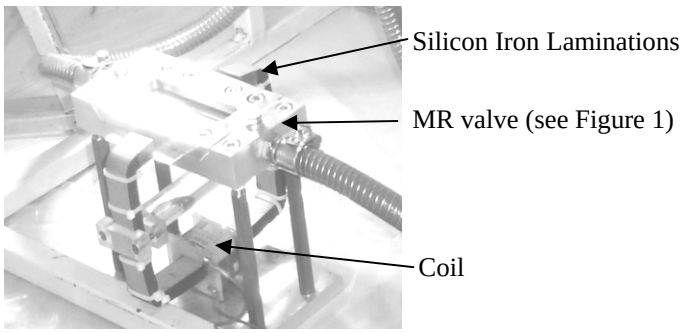

Figure 4: Assembled experimental stand

The magnetic circuit was designed in a way to provide a sufficient magnetic field to excite the MR fluid across the orifice. The magnetic circuit consisted of a magnetic core made of silicon iron and a coil (Figure 4). The main part of the core had cross section 20 mm x 10 mm (width x height) and for the part that was connected to the experimental channel, the dimensions were reduced to 20 mm x 1 mm (width x height). The coil had 140 turns and was positioned symmetrically in reference to the gap in the magnetic circuit. The magnetic excitation system was able to generate B = 0.5T between the poles. The symmetrical positioning of the coil allowed the generation of an exactly equal level of flux density on both surfaces of the poles.

The pressure gradient was generated by a piston pump, which could produce a maximum level of 2MPa. The resulting flow rates that were tested were up to 2.5×10^{-5} m^3/s.

The experiments included the following measurements: pressure signal on the inlet and outlet of the flow channel, displacement of the pump's piston, and the current applied to the coil. This was sufficient to enable the quasi-steady pressure/flow rate characteristic of the valve to be calculated.

4 MODELLING

In Section 4.1, a finite element (FE) analysis of the test facility's magnetic circuit is

performed. This enables the non-linear yield stress distribution within the valve gap to be determined. The analysis is also validated using experimental flux density measurements. In Section 4.2, a model is then derived that accounts for this non-linear yield stress distribution. This will later be compared to more simplistic models that assume a constant yield stress distribution. Consequently, the necessity to implement these more complex models will be better understood.

4.1 Magnetic field analysis

A finite element model of the magnetic circuit described in Section 3 was developed. This was built using FEMM[11] and the corresponding model is shown in Figure 5. This is a planar model, which accounts for the fill factor of the steel laminations, and the flux leakage into the surrounding air. To first validate the model, the flux density in the centre of the fluid passage was measured using a Tesla meter. These measurements were obtained in air as it is not possible to position the Tesla meter's probe in the MR fluid once the device is assembled and sealed. The fluid gap in the model (see Figure 5) was then substituted with an air gap so that the predicted flux density could be compared with the experimental readings. The results from this validation exercise are shown in Figure 6, which compares the modelled and experimental flux density values for a range of currents. In general, the correlation between model and experiment is good thus validating the FE model. There is some fluctuation in the experimental measurements although this may be attributed to the difficulties in positioning the Tesla meter's probe.

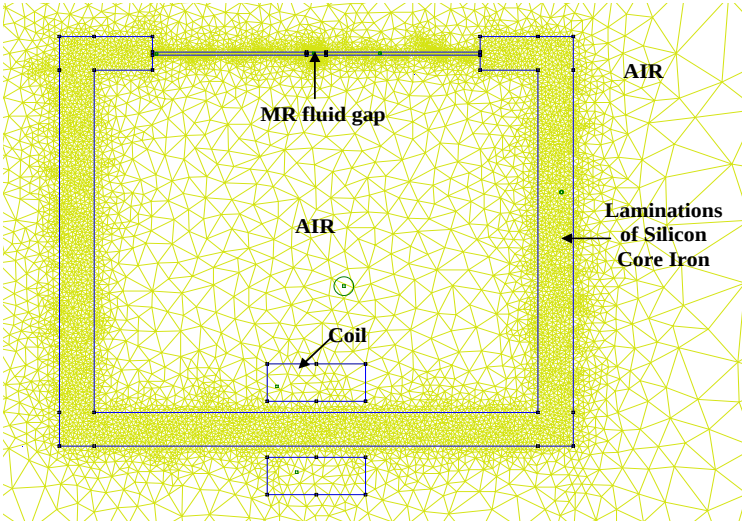

Figure 5: Finite element model of the magnetic circuit.

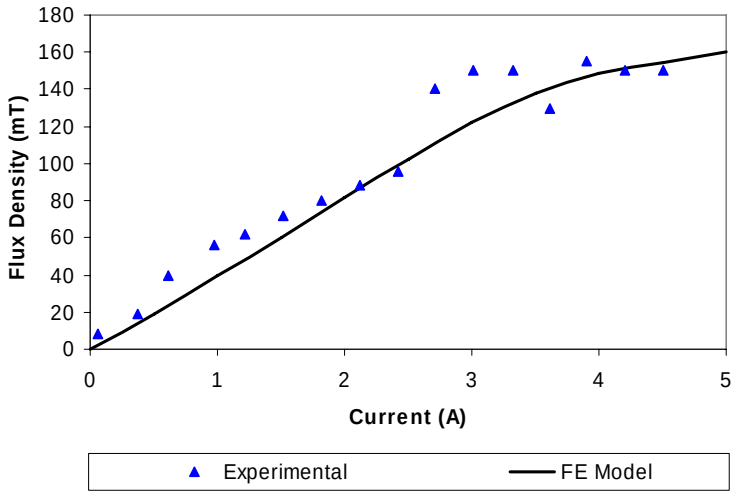

Figure 6: Experimental and theoretical flux density values in air.

The next stage is to use this validated model to predict the flux density in the MR fluid. Here, the magnetic characteristics of Fraunhofer's AD275 MR fluid[12] (i.e. the magnetic flux density versus magnetic field strength curve) was used to model the fluid passage in the FEA. Figure 7(a) shows the resulting flux density distribution, where the distance corresponds to the co-ordinate y in Figure 1(b). Clearly, the quadratic nature of this response is fairly significant. The corresponding absolute yield stress distribution is shown in Figure 7(b), which was calculated using the fluid manufacturer's yield stress versus flux density data[12]. This response can be modelled using the following quadratic formula:

$$\tau_y = ay^2 + by + c \tag{2}$$

where a, b and c are fitting constants, which are given in Table 1 for the responses shown in Figure 7(b). In the next section, MR fluid flow models are developed for the case where the MR fluid yield stress is assumed constant, and for the case where a quadratic yield stress distribution is assumed.

	Parameter		
Current	**a**	**b**	**c**
1.2A	3225436.0	-9689.0	27.2
2.4A	6767665.4	-20314.0	56.3
3.6A	9233561.7	-27721.5	69.8

Table 1: Constants for the quadratic yield stress equations.

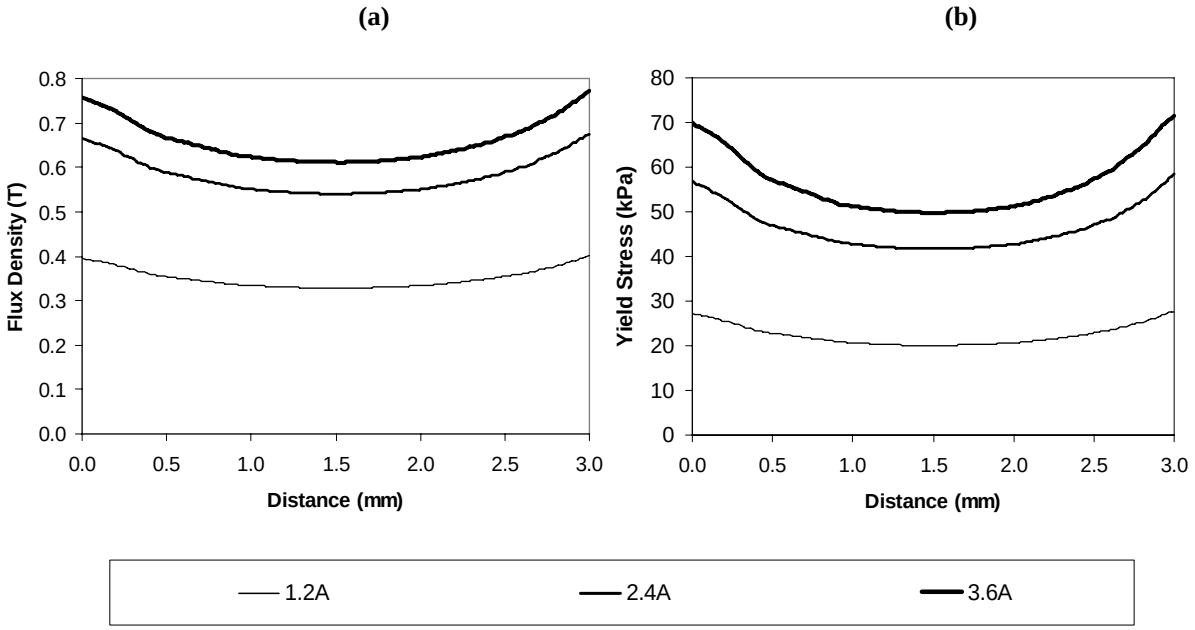

Figure 7: Predicted flux density and yield stress distributions across the valve gap. (a) Flux density and (b) yield stress.

4.2 Quasi-steady MR flow analysis

It is well know that MR fluids can be approximated as a Bingham plastic. Here, the shear stress τ within the fluid is given by:

$$\tau = \tau_y + \mu\dot{\gamma} \tag{3}$$

where τ_y is the fluid's yield stress, μ is a Newtonian viscosity component and $\dot{\gamma}$ is the shear rate. For steady Bingham plastic flow between parallel flat plates, the following Buckingham equation can be used if it is assumed that the yield stress remains constant across the gap[2] (Figure 1(a)):

$$4\left(\frac{l}{h\Delta P}\right)^3 \tau_y^3 - 3\left(\frac{l}{h\Delta P}\right)\tau_y + \left(1 - \frac{12\mu l Q}{wh^3\Delta P}\right) = 0 \tag{4}$$

where w is the breadth of the plates and all other parameters are previously defined. This

equation, which is cubic in ΔP, only has one physically meaningful root and the reader is referred to previous work for details about its solution[2, 13]. In what follows, a modified form of this Buckingham equation is derived in order to account for the quadratic yield stress distribution that was observed in Section 4.1. This will be referred to as the modified Buckingham equation.

As shown in Figure 1(b), the flow equations will be derived with respect to co-ordinate v, which represents the line of symmetry of the device. The first step is to calculate the plug width δ. This can be achieved by considering that at the plug boundary ($v = \delta/2$), the shear stress τ in the fluid is equal to the yield stress τ_y. Rewriting Equations 1 and 2 in terms of the co-ordinate v, and setting them to be equal at $v = \delta/2$ results in the following equation for shear stress:

$$\tau = \frac{\Delta P}{l} \times \frac{\delta}{2} = a\left(\frac{\delta}{2} + \frac{h}{2}\right)^2 + b\left(\frac{\delta}{2} + \frac{h}{2}\right) + c \tag{5}$$

After some manipulation, it can be shown that the plug width is given by the solution to the following quadratic equation:

$$A\delta^2 + B\delta + C = 0 \tag{6}$$

where $A = 0.5la$, $B = lah + bl - \Delta P$, and $C = l(0.5ah2 + bh + 2c)$. The only physically meaningful solution to this equation is given by:

$$\delta = \frac{-B - \sqrt{B^2 - 4AC}}{2A} \tag{7}$$

This represents the only value of plug width that is less than the valve gap height – a fundamental condition for flow to occur. The next stage is to determine the velocity profiles inside and outside of the plug. The shear rate outside of the plug is found by rearranging Equation 3, and substituting in Equations 1 and 2 (both written in terms of v):

$$\dot{\gamma} = \frac{du}{dv} = -\frac{1}{\mu}\left(\frac{\Delta P v}{l} - a\left(v + \frac{h}{2}\right)^2 - b\left(v + \frac{h}{2}\right) - c\right) \text{ for } v \geq \frac{\delta}{2} \tag{8}$$

Inside of the plug, no shearing occurs, that is:

$$\dot{\gamma} = 0 \quad \text{for } v \leq \frac{\delta}{2} \tag{9}$$

The velocity profile outside of the plug is found by integrating Equation 8, which after some manipulation gives:

$$u = -\frac{1}{\mu}\left[-\frac{av^3}{3} + \left(\frac{\Delta P}{2l} - \frac{ah}{2} - \frac{b}{2}\right)v^2 - \left(\frac{ah^2}{4} + \frac{bh}{2} + c\right)v + K\right] \tag{10}$$

where K is a constant that can be determined by substituting the boundary condition $u=0$ at $v=h/2$. This gives the following value for K:

$$K = \frac{7ah^3}{24} + \left(\frac{3b}{8} - \frac{\Delta P}{8l}\right)h^2 + \frac{ch}{2} \tag{11}$$

The velocity inside the plug is a constant and maximum, and is found by subsituting the boundary condition $u = u_{max}$ at $v = \delta/2$ into Equation 10. This gives:

$$u_{\max} = -\frac{1}{\mu}\left[-\frac{a\delta^3}{24} + \left(\frac{\Delta P}{8l} - \frac{ah}{8} - \frac{b}{8}\right)\delta^2 - \left(\frac{ah^2}{8} + \frac{bh}{4} + \frac{c}{2}\right)\delta + K\right] \tag{12}$$

where δ is given by Equation 7. Using symmetry, the volume flow rate Q across the whole channel can then be calculated as follows:

$$Q = Q_i + Q_o = w\delta u_{\max} + 2w\int_{\delta/2}^{h/2} u dv \tag{13}$$

where Q_i and Q_o are the volume flow rates inside and outside of the plug, w is the breadth of the plates, and u_{max} and u are the channel velocities given by Equations 10 and 12.

It is straightforward to formulate this model by first specifying ΔP and τ_y, and then solving for the flow rate Q. For the purpose of the present study, this was considered as an appropriate methodology. The reverse solution (to calculate ΔP given a certain Q and τ_y) is significantly more difficult to solve as the resulting equation is quartic in terms of ΔP. This requires further work, but would be useful for developing dynamic flow models and for performing time domain simulations of control systems.

The MR valve described in Section 3 also had sections that remained inactive i.e. lengths of valve that were not exposed to the magnetic field. It was straightforward to model these inactive lengths using the Newtonian equation for flow between parallel flat plates i.e. Equation 4 with $\tau_y = 0$. The inactive and active pressure drops were then summed in order to predict the total pressure drop for a given valve flow rate.

5 RESULTS

In this section, the experimental quasi-steady pressure/flow rate characteristic of the MR valve is determined. The results are then compared to the quasi-steady flow models that were developed in Section 4.2.

A typical experimental result for one constant velocity excitation is shown in Figure 8. This is shown in terms of the pressure drop versus displacement for a range of current excitations. Here, the aim is to achieve a steady state pressure drop before the end of the damper's stroke. For each current excitation, this is clearly achieved after about 40mm of displacement. The mean pressure drop in this steady state condition is then calculated and plotted against the corresponding steady-state flow rate. This process is then repeated for a range of piston velocities and current excitations in order to generate the experimental quasi-

steady pressure/flow rate curve.

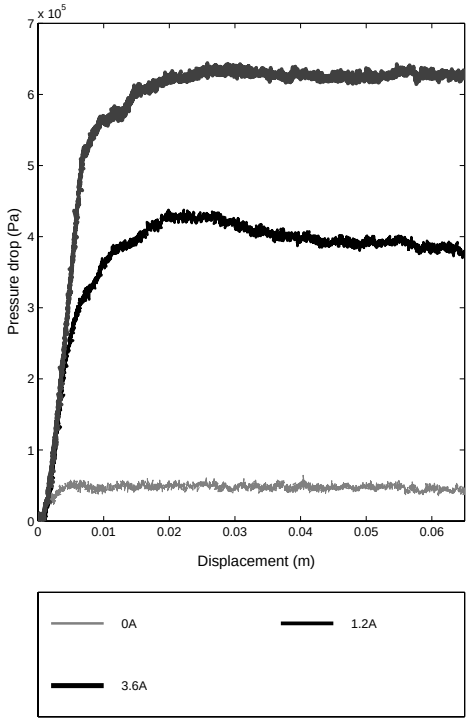

Figure 8: Pressure drop versus displacement characteristics of the MR valve.

The resulting experimental quasi-steady response is compared to the numerical models in Figure 9. Figure 9(a) first presents the numerical results obtained using the Buckingham equation, where the yield stress is assumed as constant across the valve gap (Equation 4). The value of yield stress was taken as the mean of each curve shown in Figure 7(b). Also, the viscosity used in the model was 0.7Pas, which provided a good fit with the slope of the zero-field response. This is actually higher than the value indicated by the manufacturer's data sheet, where it is possible to extrapolate a value of around 0.2Pas at comparable shear rates[12]. This discrepancy is likely to be caused by the edge effects in the MR device. For example, the model assumes that the parallel flat plates are infinitely wide such that edge effects are negligible. In the experiment, the width of the MR valve is very small thus the edge effects will be more significant, which may give rise to the larger apparent viscosity.

As shown in Figure 9(a), the Buckingham model fails to accurately predict the experimental response throughout the range of flow rates. It should be noted that at volume flow rates below about 0.4×10^{-5} m^3/s, there is a significant reduction in pressure that appears to converge towards the origin. This is due to leakage paths in the damper and so the low velocity characteristic of the MR valve cannot be accurately measured. However, this leakage does not significantly affect the results at higher velocities. This is because the resistance of the leakage paths will be significantly higher than the MR valve, thus the

volume flow rate through them will be negligible. It is therefore reasonable to concentrate on comparing the model with the experiment at flow rates beyond 0.4×10^{-5} m^3/s.

Figure 9(b) compares the experiment with the modified Buckingham equation that accounts for the quadratic yield stress distribution - the solution of Equations 6 - 13. Clearly, the correlation between model and experiment is improved, particularly for higher applied currents. Comparing Figure 9(a) with Figure 9(b), the difference between the modified and the conventional Buckingham model is particularly noticeable at higher voltages. Through inspection of Figure 7(a), this is because the range of yield stress values across the channel is greater. In summary, the modified Buckingham model will yield notable improvements in model accuracy if large variations in yield stress are anticipated.

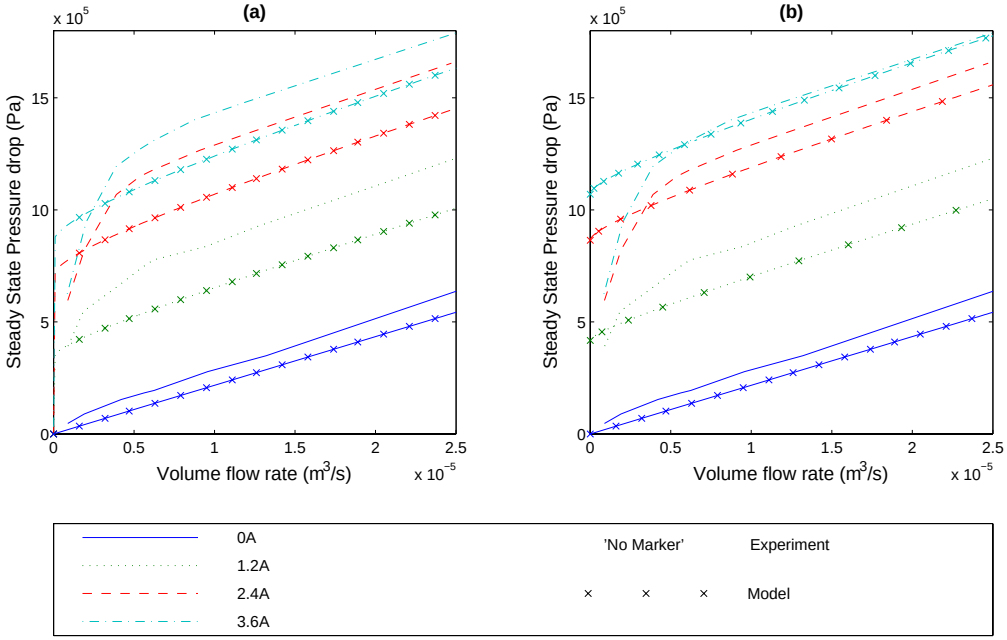

Figure 9: Comparison of the experimental quasi-steady damping function with (a) the Buckingham equation and (b) the modified Buckingham model.

6 CONCLUSIONS

This paper has investigated the performance of an MR fluid device that was found to exhibit significant variation of the magnetic flux density and hence yield stress across the valve gap. In numerical modelling, authors often neglect this effect, although the assumption is usually valid when the valve gap is small. In the present study, the valve gap was fairly large and so a more complex model that accounted for yield stress variation perpendicular to the valve gap was required.

To calculate the yield stress distribution, a finite element analysis of the magnetic circuit was performed. The FE model was first validated by using experimental flux density measurements taken in air, and then the yield stress distribution in the fluid was calculated.

The FE results indicated a significant quadratic distribution of yield stress across the valve gap.

A numerical model that accounted for this quadratic yield stress behaviour was then derived for quasi-steady Bingham plastic flow between parallel flat plates. This model was compared to quasi-steady measurements taken from the experiment, along with a simplified model that assumes a constant yield stress across the gap.

It was shown that there was a significant influence of the quadratic yield stress variation on the valve's pressure/flow rate response, and that the modified model could better account for the experimental behaviour. The model was derived to predict the flow rate given a specified valve pressure drop. The inverse of this (to predict pressure drop given flow rate) is significantly more difficult to solve and requires further work.

7 REFERENCES

1. Gavin, H P (1998), "Design method for high-force electrorheological dampers", *Smart Materials and Structures*, **7**(5), 664-673.
2. Peel, D J and Bullough, W A (1994), "Prediction of ER valve performance in steady flow", *Proceedings of the Institution of Mechanical Engineers, Part C: Journal of Mechanical Engineering Science*, **208**, 253-266.
3. Wereley, N M and Pang, L (1998), "Nondimensional analysis of semi-active electrorheological and magnetorheological dampers using approximate parallel plate models", *Smart Materials and Structures*, **7**(5), 732-743(12).
4. Goncalves, F D, Ahmadian, M, and Carlson, J D (2006), "Investigating the magnetorheological effect at high flow velocities", *Smart Materials and Structures*, **15**(1), 75-85.
5. Wereley, N M, Lindler, J, Rosenfeld, N, and Choi, Y-T (2004), "Biviscous damping behavior in electrorheological shock absorbers", *Smart Materials and Structures*, **13**(4), 743-752.
6. Wang, X and Gordaninejad, F (2000), "Flow analysis of field-controllable, electro- and magneto-rheological fluids using Herschel-Bulkley model", *Journal of Intelligent Material Systems and Structures*, **10**(8), 601-608.
7. Kavlicoglu, N C, Kavlicoglu, B M, Liu, Y, Evrensel, C A, Fuchs, A, Korol, G, and Gordaninejad, F (2007), "Response time and performance of a high torque magnetorheological fluid limited slip differential clutch", *Smart Materials and Structures*, **16**, 149-159.
8. Batterbee, D C, Sims, N D, Stanway, R, and Wolejsza, Z (2005), "Design and performance optimisation of magnetorheological oleopneumatic landing gear", *SPIE Annual International Symposium on Smart Structures and materials: Damping and Isolation*, **5760-10**.
9. Yang, G, Spencer Jr, B F, Carlson, J D, and Sain, M K (2002), "Large-scale MR fluid dampers: Modelling and dynamic performance considerations", *Engineering Structures*, **24**, 309-323.

10. Choi, Y T, Cho, J U, Choi, S B, and Wereley, N M (2005), "Constitutive models of electrorheological and magnetorheological fluids using viscometers", *Smart Materials and Structures*, **14**, 1025-1036.
11. FEMM. 2005, Foster-Miller, Inc., 350 Second Avenue, Waltham, MA 02451, USA, http://femm.foster-miller.net/index.html.
12. Bõse, H (2004), "Data sheet for AD275 MR fluid", *Personal Communication*, Fraunhofer-Institut für Silicatforschung ISC, Neunerplatz 2, D-97082 Würzburg, http://www.isc.fraunhofer.de/.
13. Sims, N D, Peel, D J, Stanway, R, Johnson, A R, and Bullough, W A (2000), "The electrorheological long-stroke damper: A new modelling technique with experimental validation", *Journal of Sound and Vibration*, **229**(2), 207-227.